Alternative model of the Antonov problem: Generalization with the presence of a mass spectrum

L. Velazquez* and S. Gómez García†
Departamento de Física, Universidad de Pinar del Río, Martí 270, Esq. 27 de Noviembre, Pinar del Río, Cuba

F. Guzmán‡
Departamento de Física Nuclear, Instituto Superior de Ciencias y Tecnología Nucleares, Carlos III y Luaces, Plaza, La Habana, Cuba
(Received 16 July 2008; published 22 January 2009)

We extend the quasiergodic model proposed as an alternative version of the Antonov isothermal model [L. Velazquez and F. Guzman, Phys. Rev. E **68**, 066116 (2003)] by including the incidence of a mass spectrum. We propose an iterative procedure inspired by the Newton-Raphson method to solve the resulting nonlinear structure equations. As an example of application, we assume the existence of a mass spectrum with a standard Salpeter form, $dN=Cdm/m^{\alpha}$. We analyze consequences of this realistic ingredient on the system thermodynamical behavior and perform a quantitative description of the mass segregation effect.

DOI: 10.1103/PhysRevE.79.011120 PACS number(s): 05.20.−y, 05.70.−a

I. INTRODUCTION

The qualitative similarities in the luminosity profiles and velocity distributions [1,2], as well as the evident similarities in the morphological structures and dynamical behaviors observed in nature [3–6], suggest the unavoidable incidence of relaxation mechanisms leading astrophysical systems at least towards quasistationary configurational stages, which could be described, in principle, by using an appropriate thermostatistical description.

Gravitation is a generic example of a self-gravitating interaction, which is not able to effectively confine particles. It is always possible that some of them may reach sufficient energy for escaping from a putative system, so that the astrophysical systems undergo an evaporation process, and therefore, they will never be in real thermodynamic equilibrium. This is precisely the origin of *long-range singularity*, which does not allow one to perform a rigorous thermodynamical description of the astrophysical systems [7,8].

The long-range singularity of the gravitational interaction is avoided in many theoretical developments by enclosing the system in a rigid container [7–16], which is a nonphysical consideration leading to isothermal distributions when the standard thermostatistical methods are considered. While this kind of model describes fairly well the basic conditions of the high condensed core of certain astrophysical structures, they are unable to describe the characteristic of their halos [18]. Obviously, consideration of the evaporation effects is a very important ingredient in order to carry out an appropriate thermostatistical description for these systems [17]. A paradigmatic example of such attempts is found in the well-known Michie-King models of globular clusters and elliptical galaxies [3–6], which show how a significant correspondence of the theoretical description with the experimental data could be reached by starting from a realistic representation of all those dynamical relaxation mechanisms acting in the underlying microscopic picture of these systems.

Following the same motivations of the Michie-King models, an alternative version of the Antonov isothermal model [7] was developed in Ref. [19]. Considering one basic assumption of the Michie-King model—the existence of tidal forces extracting out all those fast particles—the alternative model carries out the thermostatistical description starting from a *microcanonical basis*; that is, while the Michie-King models consider the binary encounters a relaxation mechanism, the alternative model assumes, instead, a *quasiergodicity* of the microscopic dynamics, an idea inspired by some recent results obtained from the study of the chaoticity of these systems [20]. For this reason, we shall hereafter refer to this alternative isothermal model as the quasiergodic model (QEM).

The main aim of the present work is to account for another realistic ingredient within this thermodynamical framework: the existence of a mass spectrum [21–23]. As expected in this context, such a background condition leads to the occurrence of *mass segregation effect*, a tendency of heavy particles to occupy the inner regions of the system displacing the lightest particles to the outer ones, which significantly affects the system behavior during its gravitational collapse. As an example of application, we shall focus on the thermodynamical description of a QEM with a Salpeter mass spectrum, a particular case with great relevance in the astrophysical context [24].

II. QEM WITH A MASS SPECTRUM

Let us consider a self-gravitating Hamiltonian system as follows:

$$H = T + U = \sum_k \frac{1}{2m_k}\mathbf{p}_k^2 - \sum_{j>k} \frac{Gm_k m_j}{|\mathbf{r}_j - \mathbf{r}_k|}, \tag{1}$$

whose quasistationary character of its dynamical evolution allows one to disregard all those macrostates where the kinetic energy of a given particle with mass m_k does not satisfy the condition

*luisberis@geo.upr.edu.cu
†sorleidis@telemail.upr.edu.cu
‡guzman@info.isctn.edu.cu

$$\frac{1}{2m_k}\mathbf{p}_k^2 + m_k\phi(\mathbf{r}_k) < m_k\phi_S, \tag{2}$$

throughout an underlying particle evaporation provoked by neighboring systems characterized here in terms of the *tidal potential* ϕ_S [18], being $\phi(\mathbf{r}_k)$ is the gravitational potential at the point $\mathbf{r}_k$ where the kth particle is located.

$$\phi(\mathbf{r}_k) = -\sum_{j\neq k}\frac{Gm_j}{|\mathbf{r}_k - \mathbf{r}_j|}. \tag{3}$$

The regularized accessible volume W_R of this system within the microcanonical ensemble is given by

$$W_R = \int_{X_R} \delta[E - H]dX, \tag{4}$$

where X_R is a subspace of the N-body phase space where condition (2) takes place, being

$$dX = C_N\prod_k (d^3\mathbf{r}_k d^3\mathbf{p}_k)/(2\pi\hbar)^3, \tag{5}$$

the volume element. (The prefactor C_N considering the particles identity will be specified below.) This integral is rewritten by using the Fourier representation of the Dirac delta function

$$W_R = \int_{-\infty}^{+\infty}\frac{dk}{2\pi}\exp(zE)\mathcal{Z}_R(z), \tag{6}$$

where

$$\mathcal{Z}_R(z) = \int_{X_R}\exp(-zH)dX \tag{7}$$

is the canonical partition function with complex argument $z=\beta+ik$, with $\beta\in R$. Integration over momenta yields

$$\int C_N\exp[-zU(\mathbf{r})]\prod_k\left(\frac{m_k}{2\pi\hbar^2 z}\right)^{3/2}\exp[\chi(\mathbf{r}_k;z)]d^3\mathbf{r}_k, \tag{8}$$

where

$$\chi(\mathbf{r}_k;z) = \ln F(\sqrt{zu_k}), \tag{9}$$

where $u_k=m_k[\phi_S-\phi(\mathbf{r}_k)]$ and $F(z)$ is defined by

$$F(z) = \mathrm{erf}(z) - \frac{2}{\sqrt{\pi}}z\exp(-z^2). \tag{10}$$

Let us suppose that the system can be divided in several classes $\{c_s\}$ of identical point particles, where n_s and m_s are the particle number and particle mass of the sth class c_s, respectively. The prefactor C_N, considering the particles identity, is given by $C_N=1/\Pi_s n_s!$. Our interest in this study is just to obtain the *mean-field approximation* appearing when the total particles number $N=\Sigma_s n_s$ of the system is very large in a way that the relative abundances $v_s=n_s/N$ can be considered fixed. This aim can be carried out by using following procedure: we partition the physical space in cells $\{\omega_\alpha\}$ and denote by $\mathbf{r}_\alpha$ the positions of their centers, and $N_s(\mathbf{r}_\alpha)$, the number of particles of the class c_s that are located inside the α cell. Introducing the particle density $n_s(\mathbf{r}_\alpha)=N(\mathbf{r}_\alpha)/v_\alpha$, where v_α is the volume of the cell ω_α, the total potential energy $U(\mathbf{r})$ can be rephrased in the mean-field approximation as follows:

$$U(\mathbf{r}) \to U[\rho,\phi] = \int_{R^3}\frac{1}{2}\rho(\mathbf{r})\phi(\mathbf{r})d^3\mathbf{r}, \tag{11}$$

where $\rho(\mathbf{r})$ is the total mass density,

$$\rho(\mathbf{r}) = \sum_s m_s n_s(\mathbf{r}), \tag{12}$$

and $\phi(\mathbf{r})$ is the Newtonian potential,

$$\phi(\mathbf{r}) = \mathcal{G}[\rho] = -\int_{R^3}\frac{G\rho(\mathbf{r}_1)d^3\mathbf{r}_1}{|\mathbf{r}-\mathbf{r}_1|}, \tag{13}$$

arising as the Green solution of the Poisson problem,

$$\Delta\phi = 4\pi G\rho. \tag{14}$$

The coordinate integration in Eq. (8) can be rephrased as follows:

$$\int\prod_s\frac{1}{n_s!}\prod_{j_s=1}^{n_s}d^3\mathbf{r}_{j_s} \simeq \prod_s\sum_{\{n_\alpha^s\}}\delta_D\left(n_s - \sum_\alpha n_\alpha^s\right)\prod_\alpha\frac{v_\alpha^{n_\alpha^s}}{n_\alpha^s!}, \tag{15}$$

by considering the division of the system in classes of identical particles $\{c_s\}$ and the partition of the physical space in cells $\{\omega_\sigma\}$, where

$$\delta_D(k) = \begin{cases}1 & \text{if } k=0\\ 0 & \text{otherwise,}\end{cases} \qquad \text{and} \qquad \sum_{\{n_\alpha^s\}} \equiv \sum_{n_1^s}\sum_{n_2^s}\cdots. \tag{16}$$

The partition function $\mathcal{Z}_R[z,\{n_s\}]$ can be rephrased by using the Stirling formula $\ln n! = n\ln n - n$ as a *functional integral* as follows:

$$\sim\int\prod_s e^{-P_s[n_s]}\delta\left[n_s - \int_{R^3}n_s(\mathbf{r})d^3\mathbf{r}\right]\mathcal{D}n_s(\mathbf{r}), \tag{17}$$

where $P_s[n_s]$ is the functional $P_s[n_s]=p_s[n_s]-\chi_s[n_s]+zU_s[n_s]$, where

$$p_s[n_s] = \int_{R^3}n_s(\mathbf{r})\left[\ln n_s(\mathbf{r}) - 1 + \frac{3}{2}\ln\left(\frac{2\pi\hbar^2 z}{m_s}\right)\right]d^3\mathbf{r}, \tag{18}$$

$$\chi_s[n_s] = \int_{R^3}n_s(\mathbf{r})\ln F\{\sqrt{zm_s[\phi_S-\phi(\mathbf{r})]}\}d^3\mathbf{r}, \tag{19}$$

$$U_s[n_s] = \frac{1}{2}\int_{R^3}m_s n_s(\mathbf{r})\phi(\mathbf{r})d^3\mathbf{r}. \tag{20}$$

It is convenient to introduce the identity

$$\int \mathcal{D}\phi(\mathbf{r})\,\delta\{\phi(\mathbf{r}) - \mathcal{G}[\rho]\} = 1 \tag{21}$$

into Eq. (17) and rewrite the delta functions by using their respective Fourier representations as follows:

$$\delta\{\phi(\mathbf{r}) - \mathcal{G}[\rho]\} \sim \int \mathcal{D}h(\mathbf{r}) \exp\left[\int_{R^3} d^3\mathbf{r} J(\mathbf{r})\{\phi(\mathbf{r}) - \mathcal{G}[\rho]\}\right], \tag{22}$$

$$\delta\left[n_s - \int n_s(\mathbf{r}) d^3\mathbf{r}\right] \sim \int_{-\infty}^{+\infty} \frac{dq_s}{2\pi} \times \exp\left[\zeta_s\left(n_s - \int_{R^3} n_s(\mathbf{r}) d^3\mathbf{r}\right)\right], \tag{23}$$

where $\zeta_s = \mu_s + iq_s$ with $\mu_s \in R$; $J(\mathbf{r}) = j(\mathbf{r}) + ih(\mathbf{r})$, a complex function with $j(\mathbf{r})$ and $h(\mathbf{r}) \in R$. The canonical partition function $\mathcal{Z}_R[z,\{n_s\}]$ is finally expressed as

$$\mathcal{Z}_R[z,\{n_s\}] \sim \int \mathcal{D}a \exp\{-\mathcal{H}[\{n_\alpha(\mathbf{r})\},\phi;z,\{n_s\},\{\zeta_s\},J]\}, \tag{24}$$

where $\mathcal{D}a \equiv \mathcal{D}\phi(\mathbf{r})\mathcal{D}h(\mathbf{r})\Pi_s \mathcal{D}n_s(\mathbf{r})dq_s$, and the functional $\mathcal{H}[\{n_\alpha(\mathbf{r})\},\phi;z,\{n_s\},\{\zeta_s\},J]$ is given by

$$\mathcal{H} = \sum_s \left\{-\zeta_s\left[n_s - \int_{R^3} n_s(\mathbf{r}) d^3\mathbf{r}\right] + P_s[n_s;z] + \int_{R^3} J(\mathbf{r})\{\mathcal{G}[m_s n_s(\mathbf{r})] - \phi(\mathbf{r})\} d^3\mathbf{r}\right\}. \tag{25}$$

It is possible to check that when N is scaled as $N \to \alpha N$ and the following scaling laws are considered:

$$\mathbf{r} \to \alpha^{-1/3}\mathbf{r}, \quad z \to \alpha^{-4/3} z, \quad \zeta_s \to \zeta_s, \quad n_s(\mathbf{r}) \to \alpha^2 n_s(\mathbf{r}),$$

$$\phi(\mathbf{r}) \to \alpha^{4/3}\phi(\mathbf{r}), \quad J(\mathbf{r}) \to \alpha^{2/3} J(\mathbf{r}), \tag{26}$$

the functional (25) behaves as $\mathcal{H} \to \alpha\mathcal{H}$. The Planck potential can be estimated for N large enough (or $\alpha \gg 1$) by using the *steepest descent method* as follows:

$$\mathcal{P}[\beta,\{n_s\}] = -\ln \mathcal{Z}_R[\beta,\{n_s\}] \simeq \max_O \min_\eta \mathcal{H}, \tag{27}$$

where $O \equiv (\{n_s(\mathbf{r})\}, \phi(\mathbf{r}))$ and $\eta \equiv (\{\mu_s\}, j(\mathbf{r}))$. The stationary conditions

$$\frac{\delta H}{\delta O} = \frac{\delta H}{\delta \eta} = 0 \tag{28}$$

lead to the following equations:

$$n_s = A^* \exp\left[-\frac{1}{2}\beta m_s \phi + m_s \mathcal{G}[j]\right] F[\sqrt{\beta m_s(\phi_S - \phi)}], \tag{29}$$

with $A^* = (m_s/2\pi\hbar^2\beta)^{3/2} \exp(-\mu_s)$ and

$$j = \sum_s n_s \left\{-\frac{1}{2}\beta m_s + \partial_\phi \ln F[\sqrt{\beta m_s(\phi_S - \phi)}]\right\}, \tag{30}$$

$$\phi = \mathcal{G}[\rho] \quad \text{and} \quad n_s = \int_{\Re^3} n_s(\mathbf{r}) d^3\mathbf{r}. \tag{31}$$

Equation (29) is conveniently rewritten by using Eq. (30) as follows:

$$n_s = C_s \exp[s(\Phi + C)] F(\sqrt{s\Phi}), \tag{32}$$

where $s = m_s/\bar{m}$, where $\bar{m}$ is the mean value of particle mass $M = N\bar{m}$, $\Phi = \beta\bar{m}[\phi_S - \phi]$, the dimensionless potential, and the constant

$$C_s = (s\bar{m}/2\pi\hbar^2\beta)^{3/2} \exp(-\mu_s - \beta s\bar{m}\phi_S). \tag{33}$$

The additional field C, hereafter referred to as the *driving function*, is given by

$$C = -\beta\bar{m}^2 \mathcal{G}[B], \tag{34}$$

where B is the function, defined as follows:

$$B = \sum_s n_s \partial_\Phi \ln F(\sqrt{s\Phi}). \tag{35}$$

It is not difficult to show that the Planck potential $\mathcal{P}[\beta,\{n_s\}]$ is given by

$$\mathcal{P} = \sum_s P_s = \sum_s p_s[n_s] - \chi_s[n_s] + \beta U_s[n_s] = -\frac{1}{2}\beta M \phi_S - \sum_s \mu_s n_s + \frac{1}{\bar{m}} \int_{\Re^3} \rho\left(\frac{1}{2}\Phi + C\right) d^3\mathbf{r}. \tag{36}$$

The entropy can be estimated from the Legendre transformation as follows:

$$S[E,\{n_s\}] \simeq \min_\beta \{\beta E[\phi;\beta,\{n_s\}] - \mathcal{P}[\beta,\{n_s\}]\}, \tag{37}$$

where $E[\phi;\beta,\{n_s\}]$ is the energy functional

$$E = \int d^3\mathbf{r} \left\{\sum_s \epsilon_s(\beta,\Phi) n_s + \frac{1}{2}\rho\phi\right\}, \tag{38}$$

and the quantity

$$\epsilon_s(\beta,\Phi) = \left[\frac{3}{2} - \Phi\partial_\Phi \ln F(\sqrt{s\Phi})\right]\frac{1}{\beta}, \tag{39}$$

the kinetic energy per particle for the s class at a given point of the system.

A nontrivial feature derived from the present analysis is the existence of the driving function C. Its presence accounts for a combined long-range correlative effect of gravitation, the evaporation, and the quasiergodic character of the microscopic dynamics, which significantly modifies the form of the particle distributions. It is very easy to check that the direct integration of a truncated Maxwell-Boltzmann distribution

$$f_{MB}(\mathbf{r},\mathbf{p}) = \begin{cases} A\exp[-\beta\varepsilon_k(\mathbf{r},\mathbf{p})], & \varepsilon_k < m_k\phi_S \\ 0, & \varepsilon_k \geqslant m_k\phi_S, \end{cases} \quad (40)$$

with $\varepsilon_k(\mathbf{r},\mathbf{p}) = \frac{1}{2m_k}\mathbf{p}_k^2 + m_k\phi(\mathbf{r})$, leads to a particle distribution of the form $\tilde{n}_s = C_s \exp[s\Phi]F(\sqrt{s\Phi})$, which obviously disregards the existence of the driving function C. In fact, the nonvanishing part of the correct distribution function associated to QEM is

$$f_{QEM}(\mathbf{r},\mathbf{p}) = A\exp\left[-\beta\left(\frac{1}{2m_k}\mathbf{p}_k^2 + m_k\varphi_{eff}(\mathbf{r})\right)\right], \quad (41)$$

where φ_{eff} is the effective potential defined by $\varphi_{eff} = \phi + \varphi_d$ with $\varphi_d = C/\beta\bar{m} = -\bar{m}\mathcal{G}[B]$.

The long-range singularity of the thermodynamical description of the astrophysical systems has been regularized in this framework since the profiles (32) and the energy per particles (39) vanish when Φ tends to zero. For Φ small, the profiles (32) drop to *quasipolytropic* distributions $n_s \propto \exp(sC)\Phi^{3/2}$ closely related to a polytropic profile with $\gamma = 5/3$. These distribution profiles correspond to an astrophysical structure exhibiting a polytropic halo, and consequently, the whole system is located inside a sphere of radius R depending on the tidal potential ϕ_S as follows:

$$\phi_S = -\frac{GM}{R}, \quad (42)$$

where M is the system total mass. The major incidence of the mass spectrum is found in the core structure. The distribution profile (32) for the s class exhibits an *isothermal character* whenever

$$F[\sqrt{s\Phi}] \simeq 1 \Rightarrow \sqrt{s\Phi} > 2.5. \quad (43)$$

This latter inequality not only clarifies that the linear size of the isothermal core is different for each class, but also that the isothermal character is mostly satisfied by the more heavy particles, which anticipate the existence of the mass segregation effect. Finally, the existence of a mass spectrum has no effect on the relevant thermodynamic limit

$$N \to \infty \text{ by keeping } \frac{E}{N^{7/3}} \text{ and } RN^{1/3} \text{ fixed}, \quad (44)$$

which is associated to the scaling laws (26).

III. NUMERICAL INTEGRATION

Our interest in this section is to develop a numerical methodology in order to obtain the spherical solutions of the present astrophysical model. We shall use the dimensionless radius $\xi = r/R$ and rephrase the constant C_s of Eq. (32) in terms of the total particle number N and the relative abundance $v_s = n_s/N$ as $C_s = Nv_sA_s/R^3$, where the new normalization constant A_s is given by

$$A_s^{-1} = \int \exp[s(\Phi + C)]F(\sqrt{s\Phi})d^3\xi. \quad (45)$$

The dimensionless potential Φ and the driving function C obey the following nonlinear Poissonian system:

$$\Delta_\xi\Phi = -4\pi\eta\Omega(\Phi,C), \quad \Delta_\xi C = -4\pi\eta\Xi(\Phi,C), \quad (46)$$

where $\Delta_\xi a = \xi^{-2}\partial_\xi(\xi^2\partial_\xi a)$, $\eta \equiv \beta GM\bar{m}/R$ (the dimensionless inverse temperature), and the functions

$$\Omega(\Phi,C) = \sum_s sv_sA_s\rho_s(\Phi,C), \quad (47)$$

$$\Xi(\Phi,C) = \sum_s sv_sA_s\zeta_s(\Phi,C), \quad (48)$$

where

$$\rho_s(\Phi,C) = \exp[s(\Phi + C)]F(\sqrt{s\Phi}), \quad (49)$$

$$\zeta_s(\Phi,C) = \exp[s(\Phi + C)]G(\sqrt{s\Phi}), \quad (50)$$

and

$$G(z) = \frac{2}{\sqrt{\pi}}ze^{-z^2}. \quad (51)$$

The mass parameter s and the relative abundance v_s describing the mass spectrum satisfy the normalization conditions

$$\sum_s v_s = 1, \quad \sum_s sv_s = 1. \quad (52)$$

Consequently, the function $\Omega(\Phi,C)$ represents a relative measure of the mass distribution that obeys the normalization condition

$$\int \Omega(\Phi,C)d^3\xi = 1. \quad (53)$$

According to its definition, the dimensionless potential Φ satisfies the boundary conditions

$$\Phi(1) = 0, \quad \Phi'(1) = -\eta. \quad (54)$$

It is possible to verify that the driving function C is determined with the precision of an arbitrary additive constant, since the continuous transformation

$$C \to C + \lambda, \quad \ln A_s \to \ln A_s - s\lambda \quad (55)$$

does not modify the nonlinear Poissonian system (46). Such symmetry possibilities to consider are the following conditions at the origin:

$$\Phi(0) = \Phi_0, \quad \Phi'(0) = 0, \quad C(0) = 0, \quad C'(0) = 0, \quad (56)$$

which guarantee the bounded character of the functions Φ and C in the whole system volume,

$$\{\Phi(\xi) < \infty, |C(\xi)| < \infty : 0 \leqslant \xi \leqslant 1\}. \quad (57)$$

Another operation of symmetry is the scaling transformation $\xi \to \bar{\xi} = \kappa\xi$, under which the functions Φ and C remain invariable.

$$\begin{pmatrix} \Phi(\xi) \\ C(\xi) \end{pmatrix} \to \begin{pmatrix} \bar{\Phi}(\bar{\xi}) = \Phi(\xi) \\ \bar{C}(\bar{\xi}) = C(\xi) \end{pmatrix}, \quad (58)$$

and the normalization constants $\{A_s\}$ and the dimensionless inverse temperature η change as follows:

$$\begin{pmatrix} A_s \\ \eta \end{pmatrix} \to \begin{pmatrix} \bar{A}_s = \kappa^{-3} A_s \\ \bar{\eta} = \kappa \eta \end{pmatrix}. \tag{59}$$

A. Iterative procedure

The numerical solution of the nonlinear Poissonian problem (46) is difficult because the normalization constants $\{A_s\}$ defining the functions Ω and Ξ are *a priori* unknown. To overcome this difficulty it is necessary to introduce a procedure that allows one to obtain these normalization constants, at least, iteratively. Let us denote this by $P_s = \eta v_s A_s$ and rewrite Eq. (46) as follows:

$$\frac{\partial G_1}{\partial \xi} = -4\pi\xi^2\Omega_0, \quad \frac{\partial \Phi}{\partial \xi} = \frac{G_1}{\xi^2},$$

$$\frac{\partial G_2}{\partial \xi} = -4\pi\xi^2\Xi_0, \quad \frac{\partial C}{\partial \xi} = \frac{G_2}{\xi^2}. \tag{60}$$

For convenience, we have introduced the functions

$$\Omega_0 = \eta\Omega = \sum_s s P_s \rho_s(\Phi, C), \tag{61}$$

$$\Xi_0 = \eta\Xi = \sum_s s P_s \zeta_s(\Phi, C), \tag{62}$$

as well as the function

$$D_0 = \sum_s P_s \rho_s(\Phi, C) = \eta D, \tag{63}$$

which is related to the total particle density D. Since the set of normalization positive constants $\{P_s > 0\}$ is unknown, our strategy is to start from an arbitrary initial set and perform the numerical integration of the problem (60) by using the initial conditions (56). In general, the dimensionless potential Φ will vanish at certain $\xi_c \neq 1$ for a given arbitrary set $\{P_s\}$, $\Phi(\xi_c) = 0$. We can use the transformations (58) and (59) in order to recover the condition $\Phi(1) = 0$ by redefining the initial set as follows:

$$P_s \to P_s^* = \xi_c^2 P_s. \tag{64}$$

The superscript $*$ denotes the quantities associated to the set $\{P_s^*\}$. Since the average mass parameter $\bar{s} = N_1^*/N_0^*$ derived from the integrals

$$N_0^* = \int_0^1 D_0 4\pi\xi^2 d\xi, \quad N_1^* = \int_0^1 \Omega_0 4\pi\xi^2 d\xi, \tag{65}$$

generally differs from the unity, the true mass parameter s^* and the effective dimensionless potential Φ^* of this mass spectrum are $s^* = s/\bar{s}$ and $\Phi^* = \bar{s}\Phi$. The corresponding relative abundance $\{v_s^*\}$ and dimensionless inverse temperature η^* are given by

$$v_s^* = \frac{P_s^*}{N_0^* A_s^*}, \quad \eta^* = \bar{s}^2 N_0^*, \tag{66}$$

where the normalization constants A_s^* are given by

$$(A_s^*)^{-1} = \int_0^1 \rho_s(\Phi, C) 4\pi\xi^2 d\xi, \tag{67}$$

which are related to the integral N_0^* as follows:

$$N_0^* \equiv \sum_s \frac{P_s^*}{A_s^*}. \tag{68}$$

As already noticed, the relative abundances in Eqs. (66) obey an implicit nonlinear dependence on the set $P^* = \{P_s^*\}$, $v_s^* = f_s(P^*)$. The problem to face is to find out a suitable set $P^* = \{P_s^*\}$ that ensures the vanishing of the *error function*

$$\delta = \frac{1}{2}\sum_s [\varphi(v_s^*) - \varphi(v_s)]^2, \tag{69}$$

where $\varphi(x)$ is a certain bijective differentiable function. The root is found by using the following iterative scheme inspired on the *Newton-Raphson method*:

$$(P_s^*)^{i+1} = (P_s^*)^i \exp\left(\theta\delta\frac{v_s}{v^2}\right), \tag{70}$$

where θ is a real parameter, $0 < \theta < 1$, $v^2 = \Sigma_s v_s^2$, and the vector component

$$v_k = -P_k^* \frac{\partial \delta}{\partial P_k^*} = -\sum_s [\varphi(v_s^*) - \varphi(v_s)] P_k^* \frac{\partial \varphi(v_s^*)}{\partial P_k^*}. \tag{71}$$

The derivatives $P_k^* \partial\varphi(v_s^*)/\partial P_k^*$ are obtained by calculating the differences of the relative abundances δv_s^* associated to a small relative change $\delta p = \delta P_k^*/P_k^*$ of the kth normalization constant. Since each one of these calculations demands the integration of the problem (60), the present iterative method is expensive in the computational sense. For this reason, we only perform in each iteration the recalculation of those normalization constants P_k^* whose relative abundances v_k^* have a significant contribution to the error function (69). We set $\theta = 0.2$, $\delta p = 10^{-5}$, and $\varphi(x) = \ln x$ and extend the above iterative procedure for each value of the parameter Φ_0 until $\delta < 5 \times 10^{-3}$. The ordinary differential equations (60) are integrated by using the fourth-order Runge-Kutta method.

B. Thermodynamic parameters and potentials

The final results derived from the numerical procedure are used to obtain the fundamental thermodynamical parameters and potentials in terms of the parameter Φ_0. The Planck potential per particle can be expressed as the sum of three different terms as follows:

$$p(\eta) = p_g + p_{ms} + p_f[\eta], \tag{72}$$

where p_g contains the contribution of the global variables N and R as follows:

$$p_g = -\frac{1}{2}\ln(NR^3) - 1 + c, \tag{73}$$

where c is an unimportant constant involving the fundamental physical units; p_{ms} accounts for the effect of the mass spectrum

$$p_{ms} = \sum_s \left(-\frac{3}{2} \ln s + \ln v_s \right) v_s, \tag{74}$$

while the terms p_f contain the contribution of the fundamental variables and the distribution profiles

$$p_f(\eta) = \frac{3}{2} \ln \eta - \frac{1}{2}\eta + \sum_s v_s \ln A_s + \int \Omega \left(\frac{1}{2}\Phi + C \right) d^3\xi. \tag{75}$$

The entropy per particle $s[u]$ is derived from $p[\eta]$ within this approximation as follows:

$$s(u) = \min_\eta \{ \eta u - p(\eta) \}, \tag{76}$$

where dimensionless energy $u = E/E_0$ with $E_0 = GM^2/R$ is given by

$$u = -\frac{1}{2} + \frac{3}{2\eta} - \frac{1}{\eta} \int \left(\frac{1}{2}\Omega + \Xi \right) \Phi d^3\xi. \tag{77}$$

Despite the fact that the present model is properly nonextensive, it admits some kind of N-independent characterization rather analogous to the one associated to the extensive systems. Even the presence of the combination NR^3 in the contribution p_g of the Planck potential per particle (73) does not affect the extensivity of this thermodynamic potential since it remains fixed in the thermodynamic limit (44). Thus, the whole thermodynamic behavior of this system is well defined in the mean-field approximation.

C. Some other observables of interest

As already discussed, the quantity $\Omega(\xi)$ characterizes the system mass distribution, while the function

$$\varphi(\xi) = -1 - \frac{1}{\eta}\Phi(\xi) \tag{78}$$

is the gravitational potential expressed in units of $\varphi_0 = GM/R$. The particle density

$$D(\xi) = \sum_s v_s A_s \rho_s(\xi) \tag{79}$$

can be combined with the expression of the kinetic energy per particle for the s class (39) in order to obtain the kinetic energy density

$$u_K = \frac{3}{2\eta} \left(D - \frac{2}{3}\Phi\Xi \right), \tag{80}$$

expressed in units of $u_0 = GM^2R^2$, which is related to the local pressure by the usual formula $p = 2u_K/3$. An interesting observable is the *isothermal function* $\gamma(\xi)$ defined as

$$\gamma(\xi) = \frac{2\eta u_K}{3D} \equiv 1 - \frac{2}{3}\Phi(\xi)\frac{\Xi(\xi)}{D(\xi)}, \tag{81}$$

which takes the value $\gamma \simeq 1$ when the distribution profile exhibits an isothermal character, so that γ could be used to study the quantitative features of the isothermal cores. The local mass spectrum

$$v_s(\xi) = \frac{1}{D(\xi)} A_n v_s \rho_s(\xi), \tag{82}$$

allows one to introduce the average mass $m(\xi)$ as follows:

$$m(\xi) = \sum_s s v_s(\xi) = \frac{\Omega(\xi)}{D(\xi)}. \tag{83}$$

These two observables can be used to characterize the mass segregation effect.

D. Mass spectrum

The consideration of a mass spectrum is a feature of the present study of QEM. Its mathematical form is actually an open question within this formalism, whose specification depends on the nature of the problem under study and it will always modify the system macroscopic behavior in some quantitative way. Due to the impossibility of performing a complete study of the admissible mathematical forms that can adopt this important background condition, we shall assume in our numerical study a mass spectrum with a standard Salpeter form as follows:

$$dv = \frac{Cdm}{m^\alpha}, \tag{84}$$

with $\alpha \simeq 2.35$ and $m \in (m_1, m_2)$, a mass spectrum with relevance in an astrophysical context [24]. Such a mass spectrum can be rewritten in terms of the relative mass parameter $s = m_s/\bar{m} \in (s_1, s_2)$ as follows:

$$dv = C_0 \frac{ds}{s^{\alpha-1}}, \tag{85}$$

where the normalization constant C_0 is given by

$$C_0 = \frac{[(1-\varepsilon^{\alpha-1})/(\alpha-1)]^{\alpha-2}}{[(1-\varepsilon^{\alpha-2})/(\alpha-2)]^{\alpha-1}}, \tag{86}$$

and the inferior s_1 and superior s_2 values are given by

$$s_1 = \frac{(1-\varepsilon^{\alpha-1})/(\alpha-1)}{(1-\varepsilon^{\alpha-2})/(\alpha-2)}, \quad s_2 = s_1/\varepsilon, \tag{87}$$

where ε is the mass ratio between the lightest and the heaviest particles of the mass spectrum, $\varepsilon = m_1/m_2$. The continuous interval $s \in (s_1, s_2)$ is approximated for a numerical study by using a set of n_c classes of identical particles, where the relative mass parameter of the nth class is given by $s_n = s_1 + (s_2 - s_1)(n-1)/(n_c - 1)$ for $n = 1, 2, \ldots, n_c$.

IV. RESULTS AND DISCUSSIONS

Before discussing the incidence of a mass spectrum on the thermodynamic description of the QEM, let us first reconsider the thermodynamic description of the QEM and the Antonov isothermal model [7] with only one class of identical particles presented in our previous paper [19]. As elsewhere discussed, the Antonov isothermal model is a very simple theoretical system that provides a direct approach to two relevant thermodynamic features of astrophysical sys-

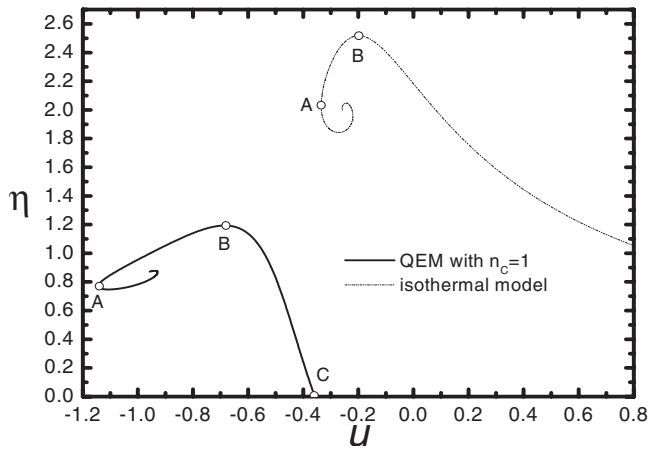

FIG. 1. Comparison between the caloric curves of the QEM and the Antonov isothermal model with only one class of identical particles.

tems: the negative heat capacities and the gravothermal collapse. However, the use of a rigid container as a way to avoid the so-called *long-range divergence* of these systems, is unrealistic. The consideration of an energy cutoff $\varepsilon_s = m_s \phi_S$ to mimic the existence of tidal forces is a more realistic ingredient that allows one to describe structures with isothermal cores and polytropic halos with a well-defined linear size characterized in terms of the tidal radius $R = GM/\phi_S$, which are features observed in globular clusters and elliptic galaxies [18].

Equation (39) of the present work amends an error in the derivation of Eqs. (39) and (40) of the previous paper [19] by disregarding the factor $\frac{1}{2}$ in the terms $\Phi \partial_\Phi \ln F(\Phi^{1/2})$ of the kinetic energy per particle $\epsilon(\beta, \Phi)$. This correction *drastically* changes the nature of the caloric curve η versus u of this astrophysical model illustrated in Fig. 1 in comparison with the one associated to the isothermal model. Notice that there is no stable equilibrium state of the QEM outside the energetic interval $u_A \leqslant u \leqslant u_C$, where $u_A = -1.14$ and $u_C = -0.36$. This qualitative character of the caloric curve differs from the corresponding caloric curve of the Antonov isothermal model, which has only an inferior bound, $u \geqslant u_A^* = -0.335$, where $u = ER_c/GM^2$, where R_c is the radius of the rigid container. This feature of the QEM is a direct consequence of the regularization prescription (2) that accounts for the effect of the particles evaporation and imposes a superior limit to the system total energy E. Apparently, the gravitation is unable to ensure a quasistationary evolution of the system when the total energy is large enough: a system initially settled in these conditions must show a strong relaxation in which it releases its excess energy by evaporation. On the other hand, the inferior limit at u_A appears as a consequence of the occurrence of the so-called *gravitational collapse* when the internal pressure of the system is unable to equilibrate the pressure of its own gravitational force.

The character of the branch AB clearly indicates the presence of macrostates with *negative heat capacities*. According to Fig. 2(a), such anomalous macrostates are unstable within the canonical ensemble, and hence, the macrostates of the branch BC with positive heat capacities are only accessed by

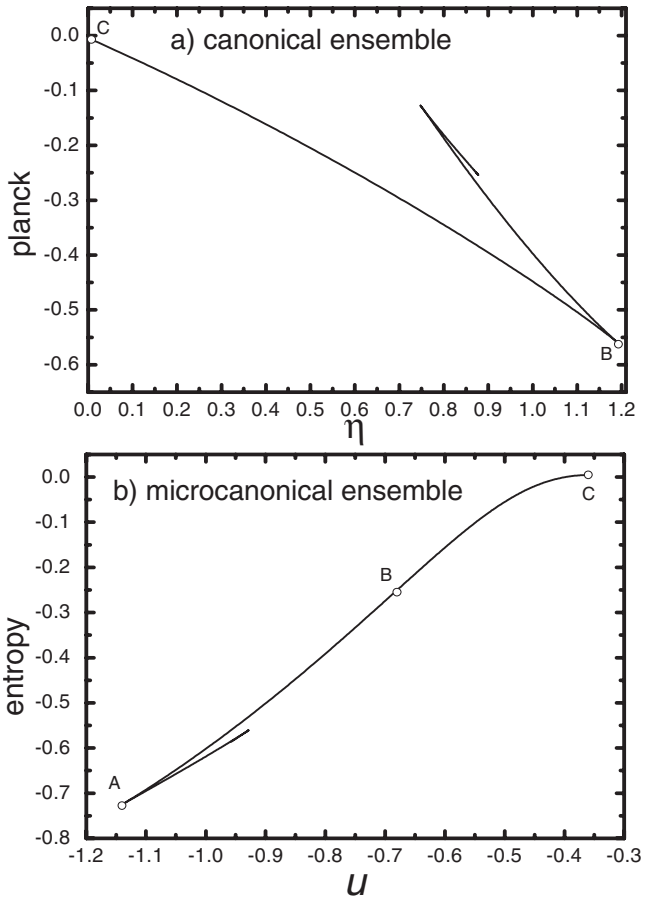

FIG. 2. Thermodynamic potentials of the QEM with only one class of identical particles. (a) Canonical ensemble: Planck thermodynamic potential per particle. (b) Microcanonical ensemble: Entropy per particle.

using this thermodynamical description (minima of the Planck potential at a given temperature). Notice also that no stable canonical macrostate of the QEM exists when $\eta > \eta_B$, with $\eta_B = 1.19$. As elsewhere discussed, this limit appears as a consequence of the occurrence of an *isothermal collapse* when the system temperature is low enough. According to Fig. 2(b), the branch ABC corresponds to stable macrostates within the microcanonical description (maxima of the entropy at a given energy), while the other branch of the spiral of the QEM illustrated in Fig. 1 is just unstable saddle points.

As already discussed in Ref. [19], the increase of the characteristic value of temperature $T_B = \eta_B^{-1}$ in QEM ($T_B = 0.84$) with respect to the one exhibited by the Antonov model ($T_B = 0.4$), is closely related to the existence of the *isothermal core*. In fact, it can be shown that the first value is not so far from the one associated to the gravitational collapse of an Antonov isothermal model with typical mass and radius of this isothermal core. In general, there is a larger particle concentration in the inner regions of the QEM than the isothermal profiles, which provokes a reduction of the gravitational potential energy. This latter fact and the obvious decrease of kinetic energy by truncation provokes a displacement of the caloric curve of QEM to negative energies shown in Fig. 1.

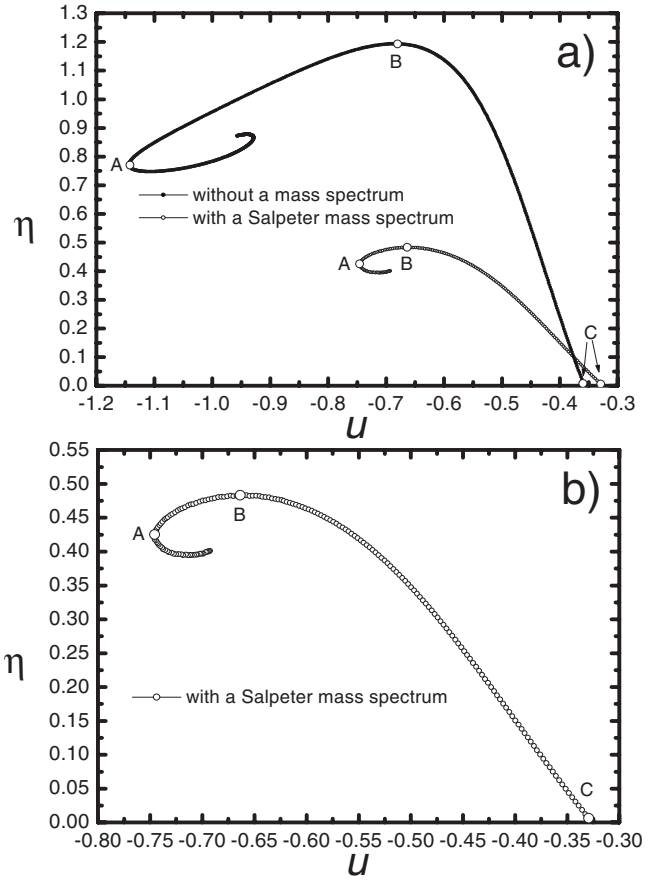

FIG. 3. Incidence of a Salpeter mass spectrum with $\varepsilon=0.1$ on the caloric curve of the QEM: (a) Comparison between the caloric curves with and without a mass spectrum; (b) a more detailed plot of the caloric curve of the QEM with a mass spectrum.

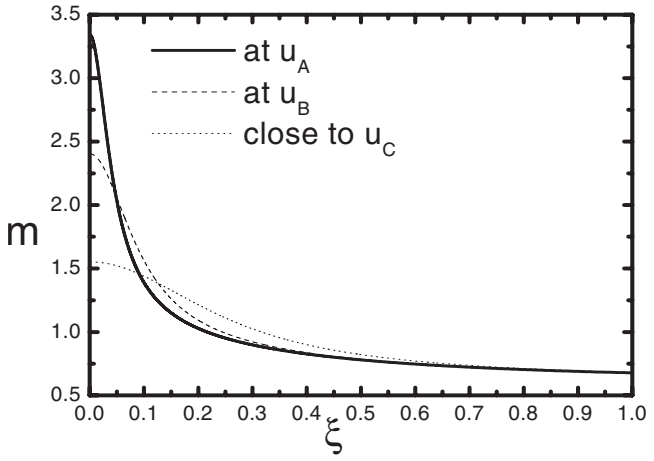

FIG. 4. The mass average function $m(\xi)$ for different energies illustrates the incidence of the mass segregation effect of the gravitational interaction, in which the heaviest particles tend to occupy the inner regions of the system, displacing the lighter particles to the outer region.

It is worth mentioning that changes in the numerical values of tidal potential ϕ_S merely modify the tidal radius of the system $R=GM/\phi_S$, and consequently, the other characteristic units of this model, such as the energy $E_0=GM^2/R$ and the temperature $T_0=GM\bar{m}/R$. The forms of all dependencies illustrated along this paper remain invariable since they are plotted by using these characteristic units.

Let us now consider the incidence of a mass spectrum on the thermodynamical description of the QEM by considering the QEM case with one class of identical particles as a reference. We assume in the present numeric study a mass spectrum obeying the Salpeter form (84) with the mass ratio value $\varepsilon=0.1$, whose continuous interval (s_1,s_2) with $s_1=0.48$ and $s_2=4.8$ is reproduced by using $n_c=50$ classes of identical particles. Besides, we are also assuming that these model systems have the same tidal radius R, total mass M, and identical number of particles N.

The caloric curve of the QEM with this mass spectrum is shown in Fig. 3. The qualitative form of the caloric curve is invariable: the inexistence of equilibrium macrostates outside a certain energetic region $u_A \leqslant u \leqslant u_C$ within the microcanonical description (from the point of the gravitational collapse u_A to the point of the system evaporation u_C), or outside the inverse temperature interval $0 \leqslant \eta \leqslant \eta_B$ within the canonical description (from the point of the system evaporation $\eta_C=0$ to the point of the isothermal collapse η_B). Thus, the consideration of a mass spectrum introduces merely quantitative changes on the characteristic values (u_X,η_X) with $X=(A,B,C)$.

The incidence of the present mass spectrum hardly modifies the characteristic energetic points u_B and u_C determining the branch of macrostates with positive heat capacities. This is not the case of the parameters associated to the gravitational collapse, u_A and η_B, which clearly experience significant changes. These observations indicate that the consideration of the mass spectrum hardly affects the energetic features of the system evaporation, but it has primordial importance in the occurrence of the gravitational collapse by reducing the values of the critical energy u_A and critical temperature $T_B=1/\eta_B$ associated to this fundamental process. Of course, it is necessary to clarify here, in order to avoid any misunderstanding, that the incidence of the mass spectrum on the system evaporation is not so important from the *equilibrium thermodynamic viewpoint*, which is not the case for the system dynamics, since the particle mass is a fundamental physical parameter affecting the evaporation rates, and consequently, the global dynamical evolution.

The mass segregation manifests as a tendency of massive particles to occupy the inner regions of the system by displacing the lighter particles to the outer zones in order to increase the mechanical stability of the system under its own gravitation. Such a behavior can be characterized by the average mass $m(\xi)$ function previously defined in Eq. (83) as well as the local mass spectrum $v_s(\xi)$ introduced in Eq. (82), whose dependences are shown in Fig. 4 for three typical energies. Figure 5 shows the average mass m_0 and all the enrichment factors $\{\omega_s\}$ at the center of the system versus the energy u, $m_0=m(0)$ and $\omega_s=v_s(0)/v_s$. These results show that the massive particles are enriched many times at the center of the system in a way such that this region is practically composed by them, with an average value close to $m_0^A \simeq 3.34$ and $m_0^B \simeq 2.40$ for the typical energies u_A and u_B, respectively.

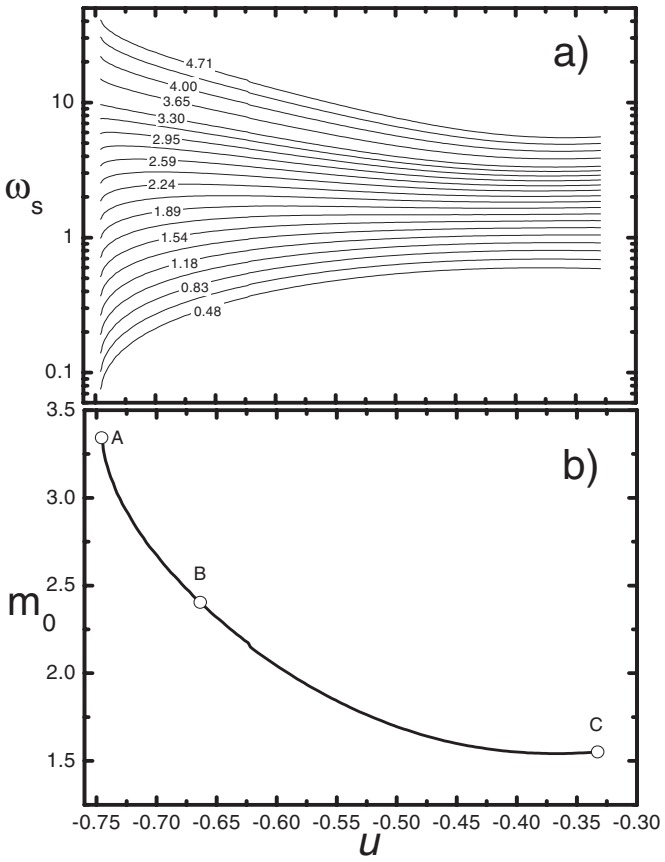

FIG. 5. Mass segregation effect illustrated in terms of (a) the mass enrichment factors $\omega_s = \nu_s(0)/\nu_s$ and (b) the average mass $m_0 = m(0)$ at the center of the system [see Eqs. (82) and (83)]. The labels in (a) indicate the corresponding dependence of the mass parameter s.

The features of the mass distribution profiles Ω for different energies are illustrated in Fig. 6. It is very interesting to notice the existence of a small region where Ω exhibits a power-law ξ^{-2} behavior for energies close to the critical point of the gravitational collapse u_A, which is a typical feature of the isothermal profiles.[1] Such a behavior indicates the presence of distribution profiles with very dense isothermal cores and diluted polytropic halos at low energies, which progressively disappear with an increasing in energy, becoming *quasipolytropic structures* [19].

In general, the quantitative description of the isothermal cores is rather imprecise as a consequence of the existence of a mass spectrum. For example, it is difficult to introduce a global indicator for the isothermal core radius. The condition (43) is only obeyed at the radius ξ by those particles whose mass parameter s belongs to the interval $s_0(\xi) \leqslant s \leqslant s_2$, where $s_m(\xi)$ is given by

[1]The Poisson-Boltzmann problem associated to the unbound isothermal model $\xi^{-2}\partial_\xi(\xi^2\partial_\xi\Phi) = -4\pi\Omega(\Phi)$ with $\Omega(\Phi) = C\exp(\Phi)$ has as a particular solution $\Phi_p(\xi) = -\ln(2\pi C) - 2\ln\xi \Rightarrow \Omega_p(\xi) = 1/2\pi\xi^2$ (corresponding to a system with infinite total mass $M \to \infty$). This power-law behavior of the mass distribution is also obeyed asymptotically for large ξ in the case of the Antonov isothermal model [7].

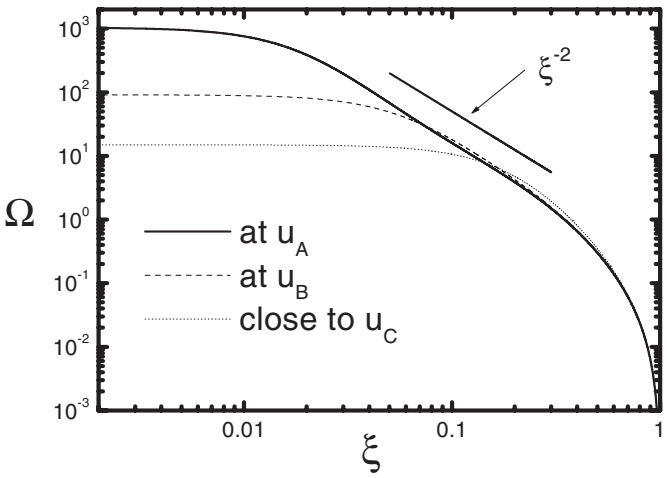

FIG. 6. Mass distribution profiles for three typical energies. Notice the presence of a region with the typical ξ^{-2} power law of the isothermal profiles close to the critical energy u_A, which indicates the existence of structures with a very dense isothermal core and diluted polytropic halos at low energies. For large energies close to u_A, the profiles are polytropic. Notice that the structure of the halos (outer system zones) is almost the same for different energies.

$$s_m(\xi) \equiv \frac{6.25}{\Phi(\xi)}. \tag{88}$$

We may be tempted to define the isothermal radius R_{ic} by the condition $s_m(R_{ic}) = s_2$; that is, when the profile of the heaviest particles lost their isothermal character. However, the mass of the heaviest particles does not account for the leading behavior of the mass distribution Ω at a given point. To this purpose the average mass function $m(\xi)$ is more adequate, so that, we assume in this study the following definition of the isothermal radius:

$$s_m(R_{ic}) = m(R_{ic}). \tag{89}$$

The isothermal core mass M_{ic} is defined as the accumulative mass at the isothermal radius R_{ic},

$$M_{ic} = \int_0^{R_{ic}} 4\pi\xi^2\Omega d\xi. \tag{90}$$

These observables are illustrated in Fig. 7. Notice that the isothermal radius vanishes at $u_{icm} \simeq -0.685$, so that the existence of a mass distribution profile with an isothermal core is only possible for configurations close to the critical point of the gravitational collapse u_A.

The reason why the presence of a mass spectrum is so important for the occurrence of the gravitational collapse can be explained in terms of the mass segregation effect. As already illustrated in Fig. 6, the mass distribution profiles for different energies mainly differ from them by the structure of their cores, since there are no appreciable differences in their halos. Hence, the features gravitational collapse is determined from the core properties, overall, the average mass of

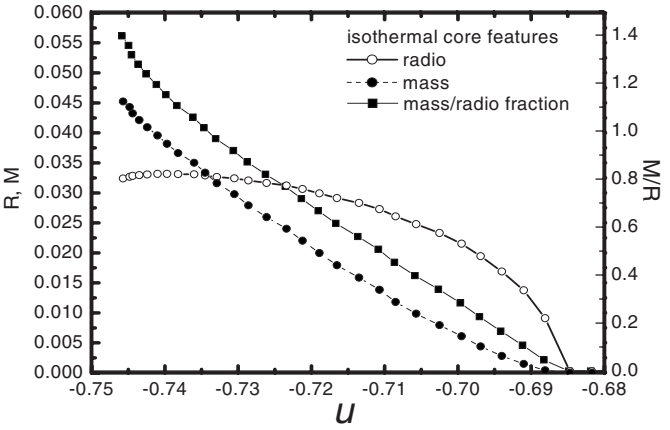

FIG. 7. Some features of the isothermal core: the mass M_{ic} and radius R_{ic} as well as the mass/radius fraction M_{ic}/R_{ic} versus the total energy u. According to these results, mass distribution profiles with an isothermal core are only admissible for energies close to the critical point of the gravitational collapse u_A.

the particles within this region. Such an idea is suggested by the fact that the inverse temperature β of the Antonov isothermal model has an inverse dependence on the mass of particles, $\beta \propto 1/m$, and therefore, an increase of this parameter as a consequence of the mass segregation effect should be the fundamental cause leading to the reduction of the typical values of the dimensionless inverse temperature η in the caloric curve shown in Fig. 3.

Let us assume that the properties of the isothermal cores can be described approximately in terms of the Antonov isothermal model [7]. Considering the total mass M and the tidal radius R, as well as the average mass particle of the system as the unity, and denoting by $(R_{ic}, M_{ic}, \bar{m}_{ic})$ the radius, the mass, and the average particle mass of the isothermal core, respectively, the critical inverse temperature of the isothermal collapse η_A can be estimated as follows:

$$\eta_A \simeq \eta_{iso} \frac{R_{ic}}{\bar{m}_{ic} M_{ic}}, \tag{91}$$

where $\eta_{iso} \simeq 2.0$ is the corresponding critical value of the Antonov isothermal model at the critical energy of the gravitational collapse (see Fig. 1). The substitution of the typical values of the isothermal core $M_{ic}/R_{ic} \simeq 1.4$ and $m_{ic} \simeq m_0^A \simeq 3.34$ yields the estimation $\eta_A \simeq 0.43$, which agrees quite well with the calculated critical value $\eta_B = 0.42$. On the other hand, the mass distribution profile at the critical point of the isothermal collapse $u_B = -0.66$ does not exhibit an isothermal core, so that, the above reasoning does not apply since the evaporation effects are significant for this particular macroscopic configuration. Nevertheless, we can estimate the critical value η_B of the isothermal collapse by assuming that this region corresponds to a QEM without a mass spectrum with a heavier particle mass $m = m_0^B$, so that, $\eta_B \simeq \eta_B^{am}/m_0^B = 0.496$, where $\eta_B^{am} = 1.19$ is the corresponding critical value of the QEM without a mass spectrum (see Fig. 3). Such a result also agrees well with the calculated value $\eta_B = 0.483$. Of course, the agreement of such simple numerical calculations cannot be overestimated, although they allow one to understand that the mass segregation is the fundamental cause explaining the changes in the caloric curve of the QEM.

V. CONCLUDING REMARKS

Although it is not fully justified in an astrophysical context, the microcanonical ensemble is more appropriate than the conventional Gibbs canonical ensemble. This ensemble allows one to consider the existence of macrostates with negative heat capacities, whose presence is crucial to explain the evolution of astrophysical systems, as well as the occurrence of the gravitational collapse, which is a fundamental process leading to the formation and structuration of the astrophysical systems in any spatial scale. The fundamental objection against using this kind of description relies on the fact that most astrophysical systems are actually open systems that undergo the influence of other systems (for example, a globular cluster under the gravitational influence of its nearby galaxy).

The present QEM accounts for, in some way, such an external influence by considering the presence of tidal interactions that lead to the existence of particle evaporation. The microscopic picture leading to the thermostatistical description is complete by considering the hypothesis that the microscopic dynamics of these systems is very chaotic to ensure the presence of certain quasistationary equilibrium in the presence of particle evaporation with an almost ergodic character [20]. According to the present results, such a quasiergodic equilibrium only takes place within a specific energetic region: from the energy of the gravitational collapse u_A to the energy of the system evaporation u_C. As already shown in this work, the main modifications introduced in this model by the incidence of a mass spectrum are directly related to the existence of the mass segregation effect.

Roughly speaking, the qualitative features of the equilibrium profiles of the QEM are quite analogous to the ones exhibited by the Michie-King models of globular clusters and elliptical galaxies [3–6]: both models describe morphological structures with high dense isothermal cores as very diluted polytropic halos, or even purely polytropic structures are also possible at high total energies. Further comparative studies between these astrophysical models are demanded in order to be precise regarding their similarities.

In addition, it would be worth clarifying if the QEM and its present extension with the inclusion of the presence of a mass spectrum could be used to fit the available experimental data of globular clusters and elliptical galaxies. Interesting cases are those astrophysical objects where the Michie-King models provide a good fitting of their structures but the incidence of binary encounters as relaxation mechanics does not provide a good explanation of its relaxation, that is, those astrophysical systems with a *collisionless evolution*. The main motivation of these studies is that the QEM does not

appeal to the binary encounters as relaxation mechanics, but the quasiergodicity of microscopic dynamics supported by the strong chaotic behavior of the astrophysical systems, whose characteristic time scale of chaoticity seems to be much smaller than the one associated to the binary encounters [20].

ACKNOWLEDGMENTS

It is a pleasure to acknowledge financial support by Grant No. PNCB-16/2004 obtained from the Cuban National Programme of Basic Sciences. L.V. thanks the financial support by FONDECYT Postdoctoral Research 3080003.

[1] J. Hjorth and J. Madsen, Mon. Not. R. Astron. Soc. **265**, 237 (1993).
[2] J. L. Sérsic, *Atlas de Galaxias Australes* (Observatorio Astronómico, Córdoba-Argentina, 1968).
[3] R. W. Michie, Mon. Not. R. Astron. Soc. **125**, 127 (1963); **126**, 331 (1963).
[4] I. A. King, Astron. J. **67**, 471 (1962); **70**, 376 (1965); **71**, 64 (1966); **71**, 276 (1966).
[5] L. Spitzer, Jr. and R. Härm, Astrophys. J. **127**, 544 (1958).
[6] S. Chandrasekhar, Astrophys. J. **98**, 54 (1943); *Principles of Stellar Dynamics* (Dover Publications Inc., New York, 1960).
[7] V. A. Antonov, Vestn. Leningr. Univ., Ser. 3: Biol. **7**, 135 (1962).
[8] D. Lynden-Bell and R. Wood, Mon. Not. R. Astron. Soc. **138**, 495 (1968); D. Lynden-Bell, *ibid.* **136**, 101 (1967).
[9] D. Ruelle, Helv. Phys. Acta **36**, 183 (1963); M. E. Fisher, Arch. Ration. Mech. Anal. **17**, 377 (1964).
[10] J. van der Linden, Physica (Amsterdam) **32**, 642 (1966); **38**, 173 (1968); J. van der Linden and P. Mazur, *ibid.* **36**, 491 (1967).
[11] W. Thirring, Z. Phys. **235**, 339 (1970).
[12] M. Kiessling, J. Stat. Phys. **55**, 203 (1989).
[13] T. Padmanabhan, Phys. Rep. **188**, 285 (1990).
[14] E. V. Votyakov, H. I. Hidmi, A. De Martino, and D. H. E. Gross, Phys. Rev. Lett. **89**, 031101 (2002).
[15] H. J. de Vega and N. Sanchez, Phys. Lett. B **490**, 180 (2000); Nucl. Phys. B **625**, 409 (2002).
[16] P. H. Chavanis, Phys. Rev. E **65**, 056123 (2002); P. H. Chavanis and I. Ispolatov, *ibid.* **66**, 036109 (2002).
[17] L. Acedo, Europhys. Lett. **73**, 698 (2006).
[18] J. Binney and S. Tremaine, in *Galactic Dynamics*, Princeton Series in Astrophysics (Princeton University Press, Princeton, NJ, 1987).
[19] L. Velazquez and F. Guzman, Phys. Rev. E **68**, 066116 (2003).
[20] P. Cipriani and M. Pettini, Astrophys. Space Sci. **283**, 347 (2003); e-print arXiv:astro-ph/0102143.
[21] K. R. Yawn and B. N. Miller, Phys. Rev. Lett. **79**, 3561 (1997); Phys. Rev. E **68**, 056120 (2003).
[22] R. T. Farouki and E. G. Salpeter, Astrophys. J. **427**, 676 (1994).
[23] J. Sopik, C. Sire, and P.-H. Chavanis, Phys. Rev. E **72**, 026105 (2005).
[24] M. J. Benacquista, www.livingreviews.org/Articles/Volume5/2002-2benacquista.